

Design, development and characterisation of novel magnesium alloys with improved corrosion resistance for medical applications

By Win Ken Look

Thesis
Submitted to Flinders University
for the degree of

Master of Engineering (Mechanical)

College of Science and Engineering
June 2024

TABLE OF CONTENTS

T/	ABLE	OF	CONTENTS	I
A	BSTR	AC1	Г	III
D	ECLA	RA1	FION	IV
Α	CKNC	WL	EDGEMENTS	V
LI	ST OI	F FIG	GURES	VI
LI	ST OI	F TA	ABLES	. VII
ΡI	JBLIC	CAT	IONS FROM THESIS	VIII
1.	INT	ROI	DUCTION	1
2.	LIT	ERA	ATURE REVIEW	2
	2.1	Intr	oduction	2
	2.2	Ма	gnesium Usage	2
	2.3	Cha	allenges of Magnesium Alloys in Biomedical Field	3
	2.4	App	proaches to Enhance Corrosion Resistance	4
	2.5	Effe	ects of Alloying Element Enhancing Magnesium	4
	2.6	Res	search Gaps & Aims	5
3.	ME	THC	DOLOGY	6
	3.1	Allo	ys Element Selection and Formulation	6
	3.2	Allo	ys Fabrication and Material Preparation	7
	3.3	Mic	rostructure Characterisation	8
	3.3.	.1	Optical Microscopy	8
	3.3.	.2	SEM & EDS.	8
	3.4	Med	chanical Properties	
	3.4.	.1	Tensile Test	8
	3.4.	.2	Hardness Test	8
	3.5	Cor	rosion Behaviours	_
	3.5.	.1	Electrochemical Measurement	
	3.5.	.2	Hydrogen Evolution Rate	9
4.	RES	SUL	TS	10
	4.1	Mic	rostructure Characterisation	
	4.1.	.1	Optical Microscopy	10
	4.1.		SEM & EDS	
	4.2		chanical Properties	
	4.2.	-	Tensile Test	
	4.2.		Hardness	
			rosion Behaviours	
	4.3.	.1	Electrochemical Measurement	14

	4.3	3.2 Hydrogen Evolution	15
	4.3	3.3 Corrosion SEM Analysis	15
5.	DIS	SCUSSION	17
į	5.1	Microstructure and Mechanical Characterisation	17
į	5.2	Corrosion Behaviour Evaluation	18
ļ	5.3	Limitations of this Study	20
6.	CO	NCLUSION & FUTURE WORK	20
(3.1	Conclusion	20
(3.2	Future Work	21
RE	FER	RENCES	22
ΑF	PEN	NDICES	26

ABSTRACT

Magnesium alloys have garnered significant attention in the biomedical field due to their potential as biodegradable implants that can reduce the need for secondary surgeries, however, their rapid corrosion remains a critical challenge. This thesis explores the development and characterisation of novel Mg-Zn-Zr-Y alloys to improve corrosion resistance and mechanical properties for biomedical applications. The research investigates six distinct alloy compositions in weight percentage (wt%): Alloy 1 (Mg-1Zn-0.5Zr-1Y), Alloy 2 (Mg-3Zn-0.5Zr-1Y), Alloy 3 (Mg-5Zn-0.5Zr-1Y), Alloy 4 (Mg-3Zn-0.25Zr-1Y), Alloy 5 (Mg-3Zn-0.75Zr-1Y), and Alloy 6 (Mg-3Zn-1Zr-1Y), focusing on their microstructural, mechanical, and electrochemical behaviours. The study began with selecting and formulating alloying elements based on extensive literature review and experimental design. Mg-Zn-Zr-Y alloys were synthesised and subjected to comprehensive characterisation using optical microscopy, scanning electron microscopy (SEM), energy dispersive spectroscopy (EDS), tensile testing, Vickers hardness testing, electrochemical testing, and hydrogen evolution testing.

Microstructural analysis revealed significant grain refinement and uniform phase distribution in Alloy 2 (Mg-3Zn-0.5Zr-1Y), attributed to the synergistic effects of Zn, Zr, and Y. This alloy demonstrated the highest ultimate tensile strength (UTS) of 201.61 MPa, a yield strength of 80.72 MPa, and a Young's modulus of 39.41 GPa, coupled with good ductility at 11.78% elongation. Despite the variations in alloy composition, the hardness values ranged narrowly, with Alloy 2 showing a slightly lower hardness of 49.2 HV compared to other alloys. Corrosion resistance was determined using open circuit potential (OCP) measurements, potentiodynamic polarisation tests, hydrogen evolution testing, and SEM analysis of corroded samples. Alloy 2 exhibited a lower corrosion current density of 1.768 μA/cm² and the most positive OCP value of -1.521 V, indicating superior resistance to corrosion initiation and propagation. Additionally, it had the lowest hydrogen evolution rate of 0.017 ml·cm²·hr⁻¹ at the 10-hour period, further confirming its excellent corrosion resistance. The findings underscore Alloy 2's potential as a viable material for biomedical applications, combining superior mechanical performance with excellent corrosion resistance.

Keywords: Magnesium alloys, Corrosion resistance, Biomedical applications, Mechanical properties, Microstructural analysis, Corrosion behaviour evaluation

DECLARATION

I certify that this thesis:

- does not incorporate without acknowledgment any material previously submitted for a degree or diploma in any university
- 2. and the research within will not be submitted for any other future degree or diploma without the permission of Flinders University; and
- to the best of my knowledge and belief, does not contain any material previously published or written by another person except where due reference is made in the text.

Thorsand
Signature of student
Print name of student Win Ken Look
Date 06/06/2024
I certify that I have read this thesis. In my opinion it is/is not fully adequate, in scope and in
quality, as a thesis for the degree of Master of Engineering (Mechanical). Furthermore, I
confirm that I have provided feedback on this thesis and the student has implemented it
minimally/partially/fully.
Signature of Principal Supervisor
Print name of Principal SupervisorReza Hashemi
Date 06/06/2024

ACKNOWLEDGEMENTS

I would like to express my deepest gratitude to my supervisor, Dr. Reza Hashemi, for his invaluable guidance and support throughout this research. I extend my heartfelt thanks to Professor Wenlong Xiao from Beihang University, Beijing, China, for fabricating the magnesium alloys used in this study. I am also profoundly grateful to Dr. Mohsen Feyzi for his guidance on the electrochemical tests. Special thanks to Tim Hodge and Matt for their assistance with samples machining, and to Dr. Alex Sibley for providing training on SEM and EDS analysis.

LIST OF FIGURES

Figure 1: Mc Bride demonstrates a method of applying Mg–Mn as a thin angled plate and screws to achieve rotation-resistant osteosynthesis [12]	
Figure 2: Corrosion of Pure Magnesium in Ringer's Solution [15] Error! Bookmark n defined.	ot
Figure 3: Pitting corrosion of Mg-Al in NaCl aqueous solution [17]	3
Figure 4: Optical microscopy images for a) Mg-1Zn-0.5Zr-1Y, b) Mg-3Zn-0.5Zr-1Y, c) Mg 5Zn-0.5Zr-1Y, d) Mg-3Zn-0.25Zr-1Y, e) Mg-3Zn-0.75Zr-1Y and f) Mg-3Zn-1Zr-1Y at 10x and 50x magnification	
Figure 5: SEM backscatter images of a) Mg-1Zn-0.5Zr-1Y, b) Mg-3Zn-0.5Zr-1Y, c) Mg-5Zn-0.5Zr-1Y,	11
Figure 6: EDS spectrum analysis of Mg-1Zn-0.5Zr-1Y	12
Figure 7: Stress-strain curves for the six Mg-Zn-Zr-Y alloys under tensile testing	13
Figure 8: Mean Vickers hardness values for the six Mg-Zn-Zr-Y alloys	14
Figure 9: a) Open circuit potential (OCP) and b) Polarisation curves for the six Mg-Zn-Zr- alloys	
Figure 10: Hydrogen evolution rates for the six Mg-Zn-Zr-Y alloys	15
Figure 11: SEM images for a) Mg-1Zn-0.5Zr-1Y and b) Mg-3Zn-0.5Zr-1Y at 200x and 800 magnification after immersing in PBS solution for 7 days.	

LIST OF TABLES

Table 1: Chemical composition (wt%) of designed magnesium alloysalloys	7
Table 2: Chemical composition of six Mg-Zn-Zr-Y alloys obtained from EDS spectrum analysis	12
Table 3: Mechanical properties of the six Mg-Zn-Zr-Y alloys based on tensile test results	
Table 4: Corrosion test results of six Mg-Zn-Zr-Y alloys.	

PUBLICATIONS FROM THESIS

The findings from this thesis have been incorporated into a manuscript, which is currently under review by my supervisor for submission as a journal article with the following details:

Look W.K., Feyzi M., Xiao W., Hashemi R. Design, development and characterisation of novel magnesium alloys with improved corrosion resistance for medical applications.

Article to be submitted to Materials and Corrosion

1. INTRODUCTION

The development of magnesium alloys for biomedical applications has drawn a lot of attention because of the distinct combination of mechanical characteristics, biocompatibility, and biodegradability. Magnesium (Mg) alloys are particularly attractive for use as bioresorbable implants in orthopaedic and cardiovascular applications because they decay naturally in the body, avoiding the need for a secondary surgery to remove the implant. This feature is complemented by their mechanical properties, which closely match those of human bone, reducing the risk of stress shielding and promoting natural bone healing processes [1].

Despite these benefits, the fast corrosion rate of magnesium in physiological environments poses a major challenge. Magnesium alloys degrade rapidly in bodily fluids, resulting in the early loss of mechanical integrity and potential adverse biological reactions due to the quick release of magnesium ions and hydrogen gas [2][3]. This issue necessitates the development of magnesium alloys with enhanced corrosion resistance without compromising their mechanical properties and biocompatibility [4][5].

Alloying is a key method for enhancing the properties of magnesium alloys. Elements like zinc (Zn), zirconium (Zr), and yttrium (Y) are known to affect the microstructure, mechanical properties, and corrosion resistance of magnesium alloys [6] [7][8]. Zinc is beneficial for strengthening and refining the grain structure of magnesium alloys, and its presence can improve corrosion resistance by forming stable and protective surface layers [1][9]. Zirconium acts as a potent grain refiner, enhancing mechanical properties and reducing corrosion rates [7][10]. Yttrium, on the other hand, is known to improve the age-hardening response and overall mechanical strength, contributing to the uniformity and stability of the microstructure [6][9].

This thesis focuses on the design, development, and characterisation of novel Mg-Zn-Zr-Y alloys with the goal of improving their corrosion resistance and mechanical properties for medical applications. The specific aims of this research include developing new magnesium alloy compositions with optimised concentrations of Zn, Zr, and Y to achieve a balance between mechanical strength and corrosion resistance. Comprehensive microstructural analysis, mechanical properties analysis, and corrosion behaviours analysis will be conducted to understand the effects of these alloying element.

2. LITERATURE REVIEW

2.1 Introduction

This literature review provides an overview of the current research on magnesium alloys in biomedical applications. It covers the usage of magnesium alloys, the challenges they face, and the strategies developed to enhance their corrosion resistance and mechanical properties. By identifying research gaps, this review aims to highlight the potential and future directions for magnesium alloys in the biomedical field.

2.2 Magnesium Usage

Magnesium alloys have garnered significant attention for their potential as resorbable bone implants, owing to their unique properties. Notably, their Young's modulus closely mimics that of natural bone, mitigating the risk of stress shielding associated with conventional metallic implants[2]. Moreover, magnesium exhibits inherent bioactivity, fostering the growth of osteoblast cells critical for bone regeneration [9].

The historical evolution of magnesium's usage in biomedical applications underscores significant milestones despite initial corrosion challenges [11]. One such milestone was the pivotal experiments conducted by Chlumsky in dogs and rabbits in the early 1900s. Chlumsky utilised magnesium sheets to prevent joint stiffness and restore joint function in both animals and humans, marking a significant advancement in the understanding of magnesium's potential in orthopaedic applications [12]. This ground-breaking research paved the way for further exploration of magnesium-based implants and their efficacy in promoting tissue regeneration and restoring physiological function.

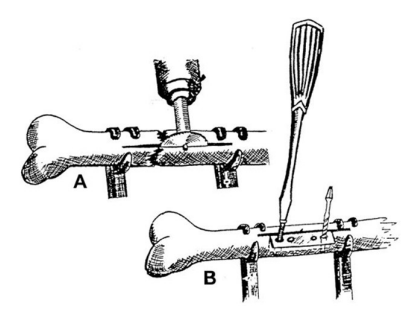


Figure 1: Mc Bride demonstrates a method of applying Mg–Mn as a thin angled plate and screws to achieve rotation-resistant osteosynthesis [12].1

¹ Reprinted from Acta Biomaterialia, Volume 6, Issue 5, F. Witte, The history of biodegradable magnesium implants: A review, Pages 1680-1692, Copyright (2010), with permission from Elsevier

2.3 Challenges of Magnesium Alloys in Biomedical Field

Magnesium alloys hold promise for biodegradable implants due to their biocompatibility and favourable mechanical properties. However, their rapid corrosion rate presents significant challenges to their widespread adoption. Pure magnesium, for instance, can degrade within the body in as little as two weeks, posing challenges, particularly in orthopaedic applications requiring extended lifespan implants [9]. Moreover, the release of hydrogen gas and magnesium ions during corrosion can trigger inflammatory responses, leading to discomfort and compromising implant effectiveness [13][14].

In physiological environments, magnesium alloys often encounter galvanic corrosion when in contact with dissimilar metals or alloys, accelerating their degradation. This phenomenon results in the release of magnesium ions, further compromising structural integrity [15]. Additionally, susceptibility to localised corrosion, especially pitting corrosion in chloride-rich environments, poses further challenges by compromising structural integrity [16].

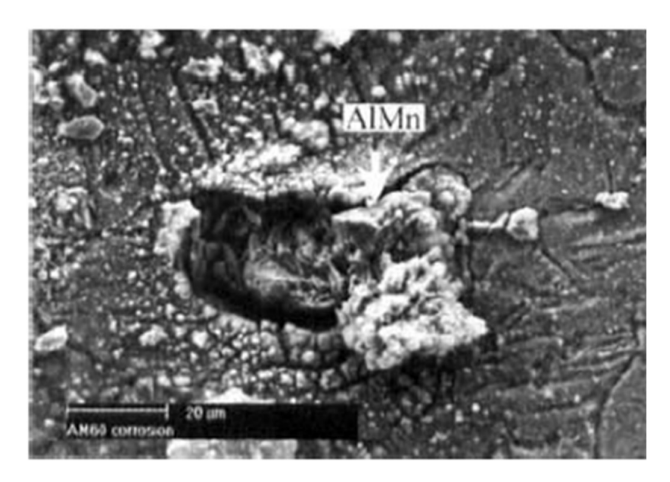


Figure 2: Pitting corrosion of Mg-Al in NaCl aqueous solution [16].²

Stress corrosion cracking (SCC) presents another significant challenge, particularly in wrought alloys, influenced by alloy composition and environmental conditions [17]. The presence of elements like aluminium and zinc can exacerbate susceptibility to SCC, especially in chloride-containing bodily fluids. Furthermore, corrosion fatigue, where crack propagation occurs under corrosive environments and mechanical stress, adds to the complexity of implant durability [18].

3

² Reprinted from Transactions of Nonferrous Metals Society of China, Volume 16, Supplement 2, R. Zeng et al., Review of studies on corrosion of magnesium alloys, Pages s763-s771, Copyright (2006), with permission from Elsevier

2.4 Approaches to Enhance Corrosion Resistance

Various strategies have been explored to enhance the corrosion resistance of magnesium alloys for biomedical applications. Surface modification techniques, such as advanced coating technologies, aim to establish protective layers against physiological corrosion, although challenges regarding delamination and long-term efficacy persist [19]. Additive manufacturing techniques, particularly 3D printing, have emerged as promising methods for crafting intricate and customised magnesium implants with enhanced mechanical properties [20]. Additionally, alloying with elements like lithium, aluminium, scandium, and rare-earth elements has been pursued to reinforce mechanical performance and improve corrosion resistance [8]. However, achieving the desired balance between corrosion resistance, mechanical properties, and biocompatibility remains a significant challenge in the development of magnesium alloys for biomedical applications.

2.5 Effects of Alloying Element Enhancing Magnesium

Aluminium (AI), calcium (Ca), zinc (Zn), manganese (Mn), zirconium (Zr), and yttrium (Y) are vital alloying elements that profoundly influence the mechanical properties and corrosion resistance of magnesium alloys. The addition of aluminium contributes to grain refinement and acts as a corrosion barrier, thereby enhancing both mechanical properties and corrosion resistance. However, higher concentrations of aluminium can lead to diminished corrosion resistance [21].

Calcium enhances microstructure refinement and biocompatibility in magnesium alloys; however, excessive calcium content may accelerate corrosion rates [22]. Zinc plays a pivotal role in strengthening magnesium alloys and improving corrosion resistance by forming benign intermetallic compounds. Nonetheless, excessive zinc content may compromise corrosion resistance [10].

Manganese aids in grain refinement and corrosion resistance by forming intermetallic compounds; nevertheless, elevated manganese levels can accelerate corrosion, necessitating precise concentration control for optimal alloy performance [8]. Zirconium enhances corrosion resistance and grain refinement in magnesium alloys, contributing to improved biocompatibility. However, careful control of zirconium concentration is essential due to potential interactions with other alloying elements [8]. Yttrium enhances corrosion resistance and mechanical properties in magnesium alloys, with lower concentrations

showing improved corrosion resistance. Excessive yttrium levels may degrade corrosion resistance, requiring further investigation for safe application in biomedical settings [23].

2.6 Research Gaps & Aims

Despite significant progress, several gaps remain in the development of corrosion-resistant magnesium alloys with optimal mechanical properties and biocompatibility. Current research has identified several critical areas that require further investigation. The exploration of novel alloying elements that can enhance both the mechanical properties and corrosion resistance of magnesium alloys is necessary. Comprehensive studies are required to elucidate the complex interactions between alloy composition and corrosion behaviour, advancing the utility of magnesium alloys in various medical applications and ensuring their effectiveness and safety for long-term use. This research aims to address these gaps by developing new magnesium alloy compositions with enhanced mechanical properties and corrosion resistance, and by investigating the complex interactions between alloy composition and corrosion behaviour. This work will contribute to the development of high-performance magnesium alloys for medical applications, advancing their practical use in the field.

3. METHODOLOGY

3.1 Alloys Element Selection and Formulation

The new magnesium alloys compositions were designed with extensive research on enhancing corrosion resistance of Mg alloys in the literature shown in Appendix i.

The formulation of new magnesium alloys was based on extensive research aimed at enhancing the corrosion resistance of Mg alloys. Detailed literature review and analysis were conducted, focusing on the values of yield strength (MPa), hydrogen evolution rate $(ml \cdot cm^{-2} \cdot h^{-1})$, corrosion potential (V), and corrosion current density $(\mu A/cm^2)$, along with biocompatibility considerations. The target values for these new magnesium alloys include achieving a yield strength exceeding the range of natural bone (51-66 MPa), attaining a Young's modulus similar to bone (17-20 GPa) [24], establishing a corrosion potential higher than the reference Mg alloy AZ91 (-1.55 V), and achieving a corrosion current density lower than that of the reference Mg alloy AZ91 (39.03 μ A/cm²) [25].

From the literature, several key studies were identified that provided valuable insights into the alloying elements most effective at improving corrosion resistance. For instance, Gungor & Incesu [3] highlighted that incorporating 3 wt% Zinc (Zn) into magnesium alloys resulted in lower corrosion rates, corrosion potentials, and corrosion currents, indicating superior corrosion resistance. Similarly, Iranshahi et al. [25] demonstrated that adding 0.5 wt% Zirconium (Zr) to magnesium alloys minimised corrosion potential and current, thereby enhancing corrosion resistance. Furthermore, Liu et al. [26] indicated that 1 wt% Yttrium (Y) contributed to reduced corrosion potential and current, further improving the corrosion resistance.

Based on these findings, 6 new alloy composition, Mg-Zn-Zr-Y, were designed with chemical composition specified in Table 1. The selection and manipulation of the wt% of Zn and Zr within the alloy aimed to study and optimise the corrosion resistance characteristics. This approach allowed for a systematic investigation of how varying the concentration of these elements affects the overall properties and performance of the magnesium alloy.

Table 1: Chemical composition (wt%) of designed magnesium alloys.

	Chemical Composition (wt%)
Alloy 1	Mg – 1Zn – 0.5Zr – 1Y
Alloy 2	Mg – 3Zn – 0.5Zr – 1Y
Alloy 3	Mg – 5Zn – 0.5Zr – 1Y
Alloy 4	Mg – 3Zn – 0.25Zr – 1Y
Alloy 5	Mg – 3Zn – 0.75Zr – 1Y
Alloy 6	Mg – 3Zn – 1Zr – 1Y

3.2 Alloys Fabrication and Material Preparation

Mg-Zn-Zr-Y alloys were synthesised by Beihang University (Beijing, China) using pure Mg (99.99 wt.%), pure Zn (99.99 wt.%), Mg-30%Zr, and Mg-30%Y master alloys. Pure Mg was initially heated in a resistance furnace to approximately 720 °C under a protective atmosphere of N_2 and SF_6 gas in a 99:1 ratio. Once the Mg was fully melted, pure Zn and the master alloys were added, and the temperature was increased to 750 °C. After complete melting of the raw materials, the melt was homogenised by mechanical stirring at 300 RPM for 3 minutes. The melt was then held at 720 °C for 20 minutes before being poured into a pre-heated steel mould at 200 °C. This process yielded Mg alloy ingots with dimensions of \emptyset 60 × 150 mm.

The as-cast alloys were sectioned into samples measuring 10 mm x 10 mm x 12 mm using a precision saw. For microstructural characterisation, the samples were hot mounted with 20 ml of MultiFast using a Struers CitoPress-15. The mounted samples underwent a series of polishing steps with a Struers Tegramin-25. Initially, plane grinding was performed using 320 grit SiC-Foil, followed by polishing with an MD-Largo disc and 9 μ m diamond abrasive. Subsequent finer polishing utilised an MD-Mol disc with 3 μ m diamond abrasive, and final mirror polishing was achieved using an MD-Chem disc with 0.25 μ m Oxide Polishing Suspension Non Dry (Appendix ii).

For corrosion experiments, the samples were sanded sequentially on all surfaces with 120, 240, 400, 600, and 1200 grit sandpaper to achieve a uniform surface finish, ensuring the accuracy of subsequent testing.

3.3 Microstructure Characterisation

3.3.1 Optical Microscopy

The microstructural analysis of the polished samples was conducted at Flinders University (Adelaide, SA, Australia) using a Zeiss Axio Imager Z2 optical microscope. Samples were prepared and polished to achieve a mirror-like finish, ensuring clear and detailed observations. The microscope was used to capture high-resolution images of the microstructure, enabling the identification of grain boundaries, phases, and other microstructural features pertinent to the characterisation of the Mg alloys. Multiple areas of each sample were examined to ensure representative and reliable microstructural data.

3.3.2 **SEM & EDS**

The microstructures of the developed magnesium alloys were analysed using a Scanning Electron Microscope (SEM) at Flinders Microscopy and Microanalysis (Adelaide, SA, Australia). The SEM used was an FEI Inspect F50, equipped with an EDT secondary electron detector, a concentric backscatter electron detector, and an Ametek EDAX Energy Dispersive Spectroscopy (EDS) detector.

Prior to SEM and EDS analysis, the samples were mirror-polished as outlined in Section 0. SEM imaging was conducted with a working distance of 10 mm, an accelerating voltage of 30 kV, and a spot size of 5 nm.

3.4 Mechanical Properties

3.4.1 Tensile Test

Tensile testing was conducted at Flinders University (Adelaide, SA, Australia) on dog bone specimens, which were prepared with a gauge length of 50 mm, a width of 12.5 mm, and a thickness of 3 mm in accordance with ASTM E8M-01 standards. These specimens were cut from the Mg alloys ingots. The tensile tests were carried out using an Instron Tensile Tester at a displacement rate of 1.5 mm/min and at room temperature. An extensometer was employed to accurately measure the strain of the specimens.

3.4.2 Hardness Test

Hardness testing was performed at Flinders University (Adelaide, SA, Australia) using a Vickers hardness testing machine (Struers DuraScan-20) with a testing load of HV 0.5 (4.903 N) and a dwell time of 10 seconds at room temperature. Each sample underwent

eight measurements to ensure the accuracy and consistency of the hardness values obtained.

3.5 Corrosion Behaviours

3.5.1 Electrochemical Measurement

Electrochemical testing was performed at Flinders University (Adelaide, SA, Australia) in a controlled chamber using a standard three-electrode setup. The magnesium alloy sample, with an exposed area of 1 cm², served as the working electrode. An Ag/AgCl electrode was used as the reference electrode, and a platinum foil functioned as the counter electrode.

To mimic physiological conditions, the samples were immersed in a phosphate-buffered saline (PBS) solution. The corrosion behaviour of the samples was analysed using an Autolab PGSTAT204 potentiostat. The testing procedure began with an open circuit potential (OCP) measurement for 1 hour to establish a stable baseline. After the OCP measurement, polarization tests were carried out at a scan rate of 0.8 mV/s over a potential range of ±0.3 V relative to the OCP [27].

The resulting corrosion potentials and corrosion current densities were recorded and presented graphically to illustrate the electrochemical performance of the magnesium alloys. This data provided insights into the corrosion resistance and overall electrochemical stability of the samples.

3.5.2 Hydrogen Evolution Rate

Samples with recorded total surface areas were immersed in PBS solution within a conical flask at Flinders University (Adelaide, SA, Australia). An inverted graduated cylinder, also filled with PBS, was positioned over the samples to collect the released hydrogen gas.

To ensure consistent conditions, the ratio of PBS solution volume (ml) to sample surface area (cm²) was maintained at 25:1. During the measurement process, the graduated cylinder was slightly tilted to prevent hydrogen gas from adhering to the cylinder walls. The volume of hydrogen gas collected was recorded hourly over a 10-hour period.

The hydrogen evolution rate (HER) was calculated using the following formula:

$$HER = \frac{V}{ST} \left(ml \cdot cm^{-2} \cdot h^{-1} \right) \tag{1}$$

where V is the volume of hydrogen evolved, T is the immersion time and S is the exposed surface area of the sample [28].

4. RESULTS

4.1 Microstructure Characterisation

4.1.1 Optical Microscopy

The microstructures obtained for polished Mg-Zn-Zr-Y alloys by optical microscopy are depicted in Figure 3. Alloy 1 (Mg-1Zn-0.5Zr-1Y) consists of larger and more irregular grains, with an average grain size of approximately 108 µm. Alloy 2 (Mg-3Zn-0.5Zr-1Y) displays more refined and uniformly distributed grains, with an average grain size of about 101 µm. In contrast, Alloy 3 (Mg-5Zn-0.5Zr-1Y) shows further refinement with higher zinc content, but the grain size distribution becomes heterogeneous, ranging from 70 to 140 µm. Alloy 4 (Mg-3Zn-0.25Zr-1Y) presents moderately refined grains, but the microstructure reveals distinct phase appearances that are not as uniform as in the other alloys. Alloy 5 (Mg-3Zn-0.75Zr-1Y) displays well-refined grains, indicating that increasing the Zr content beyond 0.5% further improves grain refinement. Finally, Alloy 6 (Mg-3Zn-1Zr-1Y) shows uniformly fine grains, suggesting that higher Zr content continues to enhance grain refinement.

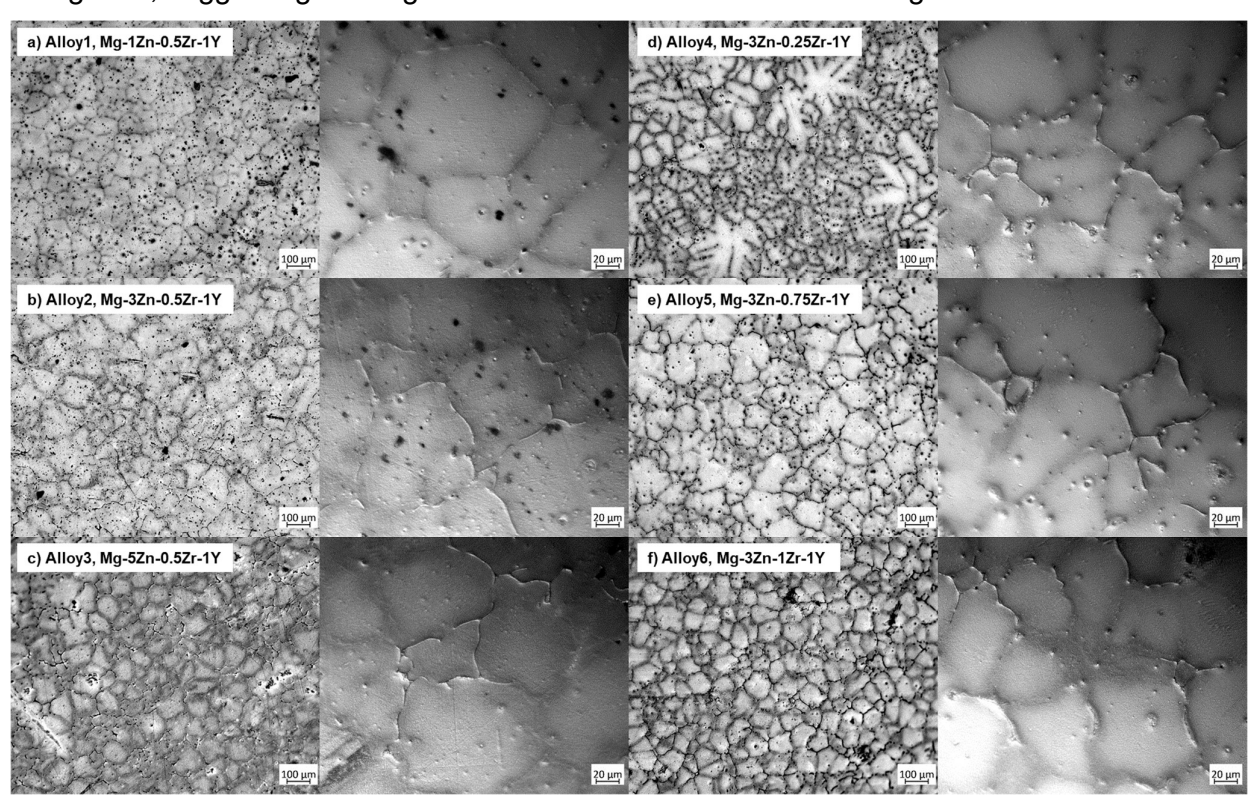


Figure 3: Optical microscopy images for a) Mg-1Zn-0.5Zr-1Y, b) Mg-3Zn-0.5Zr-1Y, c) Mg-5Zn-0.5Zr-1Y, d) Mg-3Zn-0.25Zr-1Y, e) Mg-3Zn-0.75Zr-1Y and f) Mg-3Zn-1Zr-1Y at 10x and 50x magnification.

4.1.2 SEM & EDS

The SEM images and EDS analysis provide detailed insights into the microstructural features and elemental composition of the Mg-Zn-Zr-Y alloys. Generally, the darker regions in these alloys correspond to the α-Mg matrix while the lighter regions indicate the presence of intermetallic compounds such as Mg-Zn, Mg-Zr, and Mg-Y phases. Figure 4 shows that Alloy 1 (Mg-1Zn-0.5Zr-1Y) exhibits coarse intermetallic phases along the grain boundaries, indicating less effective grain refinement and larger grain sizes. In contrast, Alloy 2 (Mg-3Zn-0.5Zr-1Y) displays finer intermetallic phases with a more uniform distribution. Alloy 3 (Mg-5Zn-0.5Zr-1Y) demonstrates further refinement with higher Zn content but a heterogeneous distribution of phases is observed. Alloy 4 (Mg-3Zn-0.25Zr-1Y) has moderately refined grains with distinct phase appearances. Alloy 5 (Mg-3Zn-0.75Zr-1Y) shows well-refined grains, and Alloy 6 (Mg-3Zn-1Zr-1Y) exhibits uniformly fine grains with a high density of intermetallic phases. The EDS spectrum analysis provides a detailed examination of the elemental composition of the six developed Mg-Zn-Zr-Y alloys (Figure 5). Table 2 summarises the chemical composition of the six Mg-Zn-Zr-Y alloys from EDS analysis, with detailed spectra provided in Appendices Appendix iii and Appendix iv.

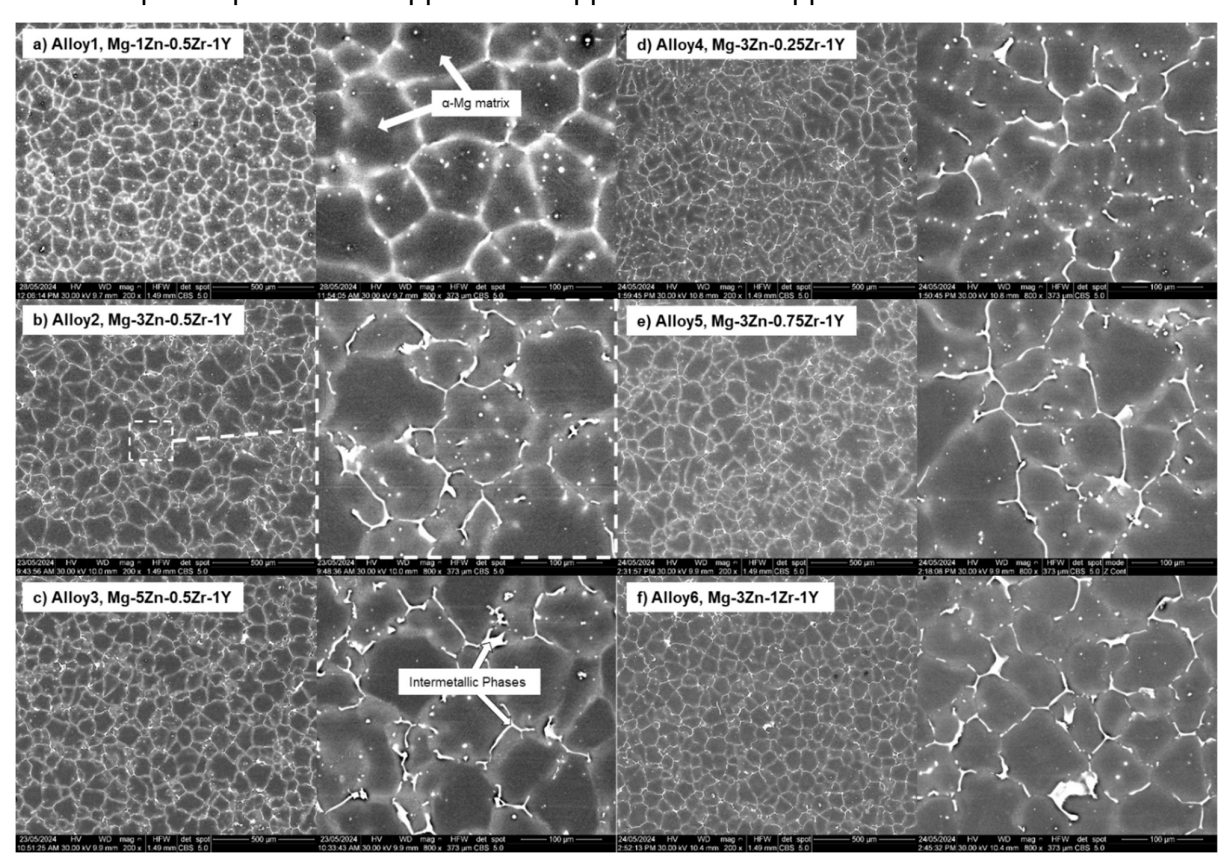


Figure 4: SEM backscatter images of a) Mg-1Zn-0.5Zr-1Y, b) Mg-3Zn-0.5Zr-1Y, c) Mg-5Zn-0.5Zr-1Y, d) Mg-3Zn-0.25Zr-1Y, e) Mg-3Zn-0.75Zr-1Y and f) Mg-3Zn-1Zr-1Y at 200x and 800x magnifications.

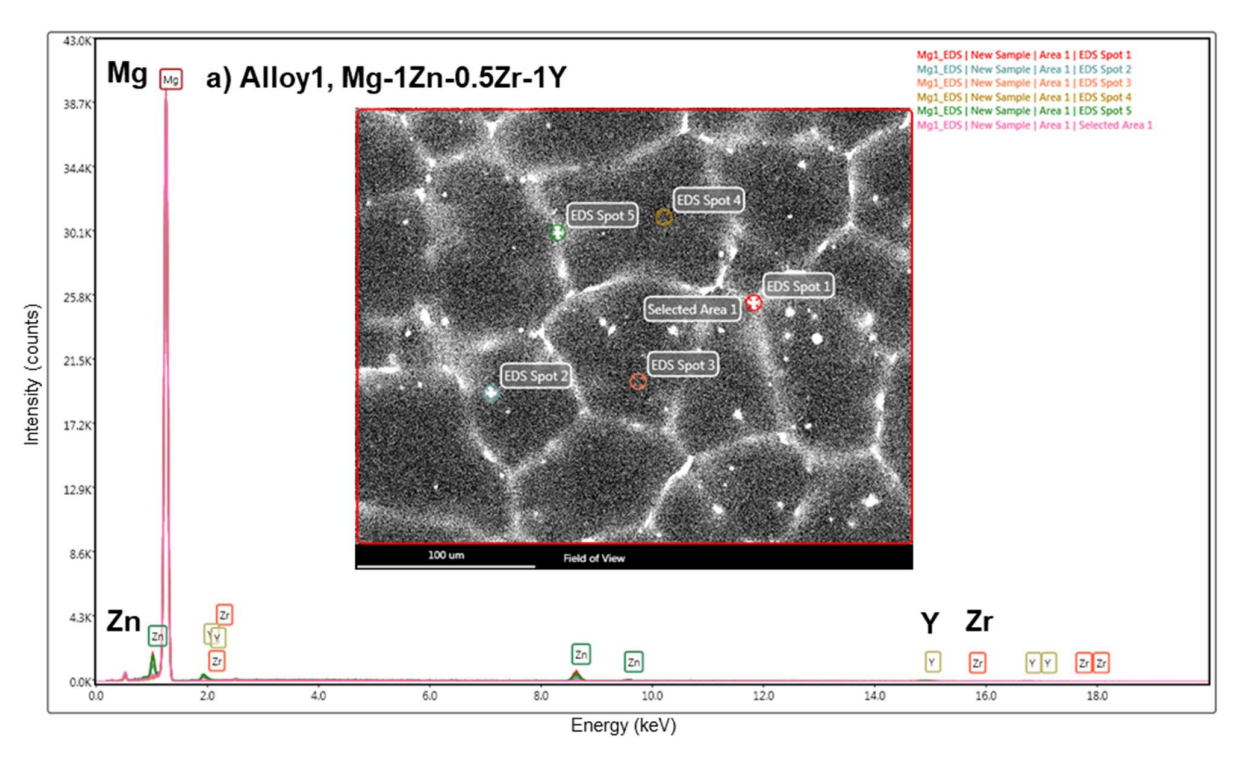


Figure 5: EDS spectrum analysis of Mg-1Zn-0.5Zr-1Y.

Table 2: Chemical composition of six Mg-Zn-Zr-Y alloys obtained from EDS spectrum analysis.

Floment	Alloy 1	Alloy 2	Alloy 3	Alloy 4	Alloy 5	Alloy 6
Element (wt%)	(Mg-1Zn-	(Mg-3Zn-	(Mg-5Zn-	(Mg-3Zn-	(Mg-3Zn-	(Mg-3Zn-
(WL70)	0.5Zr-1Y)	0.5Zr-1Y)	0.5Zr-1Y)	0.25Zr-1Y)	0.75Zr-1Y)	1Zr-1Y)
Mg	97.11	95.48	93.93	96.42	96.33	96.00
Zn	1.65	3.15	4.94	2.57	2.17	2.42
Zr	0.53	0.50	0.32	0.23	0.74	0.83
Y	0.71	0.87	0.81	0.78	0.76	0.75

4.2 Mechanical Properties

4.2.1 Tensile Test

The tensile test results for the six developed Mg-Zn-Zr-Y alloys are illustrated in Figure 6 and summarised in Table 3, reveal significant variations in mechanical properties influenced by their respective compositions. Alloy 1 (Mg-1Zn-0.5Zr-1Y) shows moderate mechanical strength and ductility with a yield strength of 71.75 MPa and an elongation of 10.38%. Alloy 2 (Mg-3Zn-0.5Zr-1Y) stands out with superior mechanical properties, demonstrating the highest ultimate tensile strength (UTS) of 201.61 MPa and an elongation of 11.78%. Alloy 3 (Mg-5Zn-0.5Zr-1Y) achieves the highest yield strength of 88.56 MPa and Young's modulus of 42.87 GPa but has reduced ductility with an elongation of 4.17%. Alloy 4 (Mg-3Zn-0.25Zr-

1Y) exhibits lower yield strength (68.42 MPa) and UTS (151.14 MPa). Alloy 5 (Mg-3Zn-0.75Zr-1Y) shows improved yield strength (82.30 MPa) and UTS (177.36 MPa). Alloy 6 (Mg-3Zn-1Zr-1Y) maintains high strength with a yield strength of 80.98 MPa and a Young's modulus of 40.85 GPa but has an elongation of 7.10%.

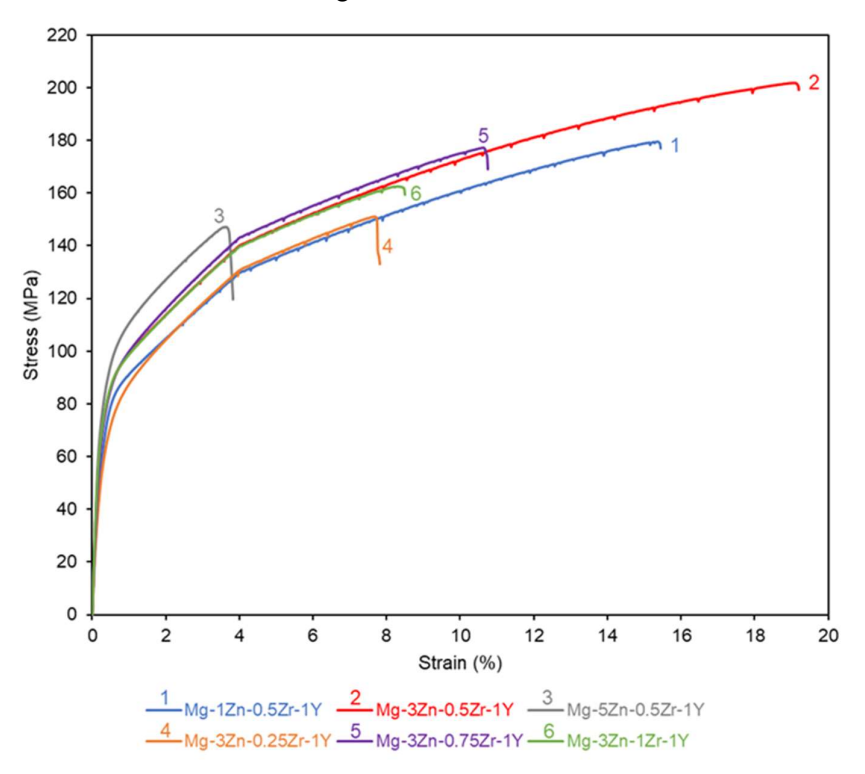


Figure 6: Stress-strain curves for the six Mg-Zn-Zr-Y alloys under tensile testing.

Table 3: Mechanical properties of the six Mg-Zn-Zr-Y alloys based on tensile test results.

Alloys	Yield Strength (MPa)	Young's Modulus (GPa)	UTS (MPa)	Elongation (%)
1) Mg-1Zn-0.5Zr-1Y	71.75	28.37	179.41	10.38
2) Mg-3Zn-0.5Zr-1Y	80.72	39.41	201.61	11.78
3) Mg-5Zn-0.5Zr-1Y	88.56	42.87	147.00	4.17
4) Mg-3Zn-0.25Zr-1Y	68.42	27.51	151.14	8.67
5) Mg-3Zn-0.75Zr-1Y	82.30	33.15	177.36	7.00
6) Mg-3Zn-1Zr-1Y	80.98	40.85	162.6	7.16

4.2.2 Hardness

The hardness values for the six Mg-Zn-Zr-Y alloys shown in Figure 7 generally fall within a narrow range of approximately 48.6 HV to 51.5 HV. Alloy 1 (Mg-1Zn-0.5Zr-1Y) and Alloy 4 (Mg-3Zn-0.25Zr-1Y) exhibit hardness values of 51.0 HV and 51.5 HV respectively. Alloy 2

(Mg-3Zn-0.5Zr-1Y) has a hardness of 49.2 HV. Alloy 3 (Mg-5Zn-0.5Zr-1Y) demonstrates a hardness value of 51.2 HV. Alloy 5 (Mg-3Zn-0.75Zr-1Y) exhibits a hardness of 50.8 HV. Lastly, Alloy 6 (Mg-3Zn-1Zr-1Y) shows the lowest hardness value of 48.6 HV.

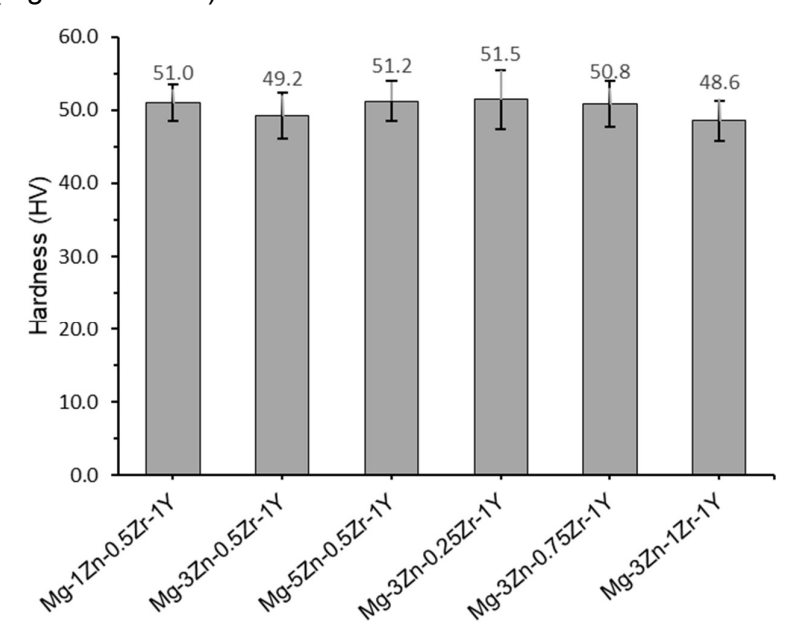


Figure 7: Mean Vickers hardness values for the six Mg-Zn-Zr-Y alloys.

4.3 Corrosion Behaviours

4.3.1 Electrochemical Measurement

The open circuit potential (OCP) measurements for the six Mg-Zn-Zr-Y alloys provide insights into the electrochemical stability of these materials. Alloy 1 (Mg-1Zn-0.5Zr-1Y) exhibits a lowest stabilised OCP value of -1.552 V, indicating that it is the least corrosion-resistant among the tested alloys. Alloy 2 (Mg-3Zn-0.5Zr-1Y) shows the most positive stabilised OCP value of -1.521 V, indicating higher corrosion resistance. Alloy 3 (Mg-5Zn-0.5Zr-1Y) has a stabilised OCP value of -1.527 V. Alloy 4 (Mg-3Zn-0.25Zr-1Y) exhibits a stabilised OCP value of -1.540 V. Alloy 5 (Mg-3Zn-0.75Zr-1Y) and Alloy 6 (Mg-3Zn-1Zr-1Y) exhibit stabilised OCP values of -1.547 V and -1.529 V respectively (Figure 8a).

The potentiodynamic polarisation curves for the six Mg-Zn-Zr-Y alloys show Alloy 1 (Mg-1Zn-0.5Zr-1Y) has a corrosion current density of 4.079 μ A/cm², indicating a higher corrosion rate. Alloy 2 (Mg-3Zn-0.5Zr-1Y) exhibits a lower current density of 1.768 μ A/cm², demonstrating superior corrosion resistance. Alloy 3 (Mg-5Zn-0.5Zr-1Y) has the highest current density at 14.436 μ A/cm². Alloy 4 (Mg-3Zn-0.25Zr-1Y) shows a moderate current density of 2.118 μ A/cm². Alloys 5 (Mg-3Zn-0.75Zr-1Y) and 6 (Mg-3Zn-1Zr-1Y) exhibit current density values of 7.098 μ A/cm² and 1.023 μ A/cm² respectively (Figure 8b).

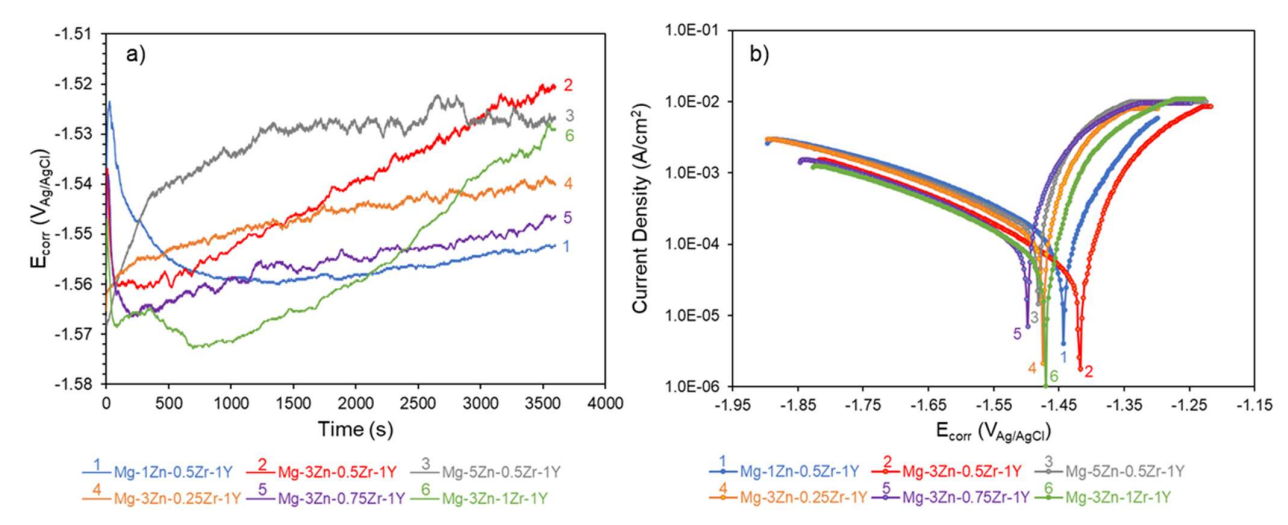


Figure 8: a) Open circuit potential (OCP) and b) Polarisation curves for the six Mg-Zn-Zr-Y alloys.

4.3.2 Hydrogen Evolution

The hydrogen evolution rate measurements in Figure 9 for the six Mg-Zn-Zr-Y alloys provide further insight into their corrosion behaviours. Alloy 1 (Mg-1Zn-0.5Zr-1Y) exhibits the highest hydrogen evolution rate, reaching up to 0.237 ml·cm²·hr⁻¹. Alloy 2 (Mg-3Zn-0.5Zr-1Y) shows the lowest hydrogen evolution rate, as low as 0.017 ml·cm²·hr⁻¹ at 10-hour period. Alloys 3 (Mg-5Zn-0.5Zr-1Y), 4 (Mg-3Zn-0.25Zr-1Y), 5 (Mg-3Zn-0.75Zr-1Y), and 6 (Mg-3Zn-1Zr-1Y) exhibit intermediate hydrogen evolution rates.

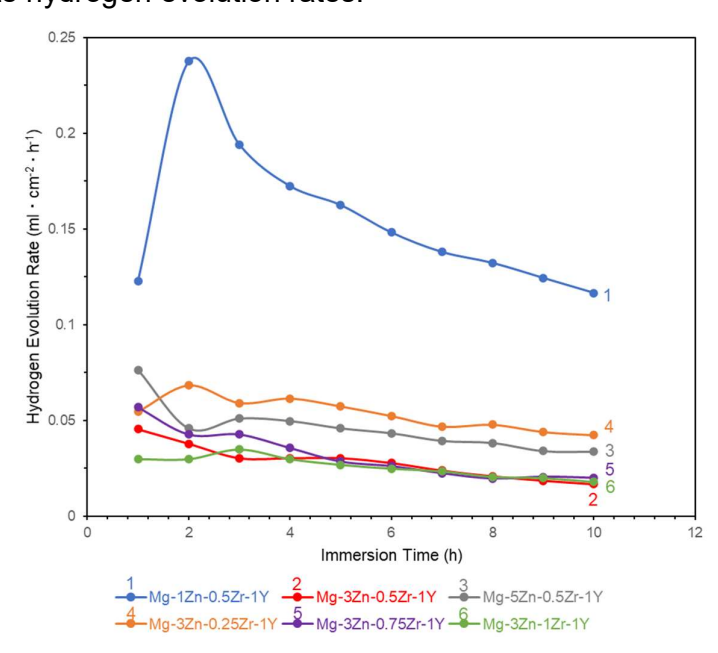


Figure 9: Hydrogen evolution rates for the six Mg-Zn-Zr-Y alloys.

4.3.3 Corrosion SEM Analysis

The SEM analysis of corroded Alloy 1 (Mg-1Zn-0.5Zr-1Y) and Alloy 2 (Mg-3Zn-0.5Zr-1Y) was performed after immersion in PBS solutions for 7 days (refer to Appendix vi for actual photos). The selection of these alloys, representing the lowest and highest corrosion

resistance, is based on the electrochemical and hydrogen evolution testing results. In the actual photos shown in Appendix vi, Alloy 1 shows significant white corrosion products, indicating more severe corrosion. Alloy 2 displays fewer corrosion products, suggesting better corrosion resistance.

In Figure 10, the SEM images of Alloy 1 reveal extensive needle-like corrosion products and a porous surface, indicative of severe chemical reactions and corrosion. The higher density of corrosion products and their irregular distribution confirm the higher corrosion rate observed in electrochemical tests. In contrast, the SEM images of Alloy 2 show a more stable and uniform surface with fewer needle-like structures. The surface appears less porous and more intact, correlating with the lower corrosion rates indicated by the hydrogen evolution and electrochemical testing. This suggests that Alloy 2 has better corrosion resistance, forming more protective and stable corrosion products compared to Alloy 1.

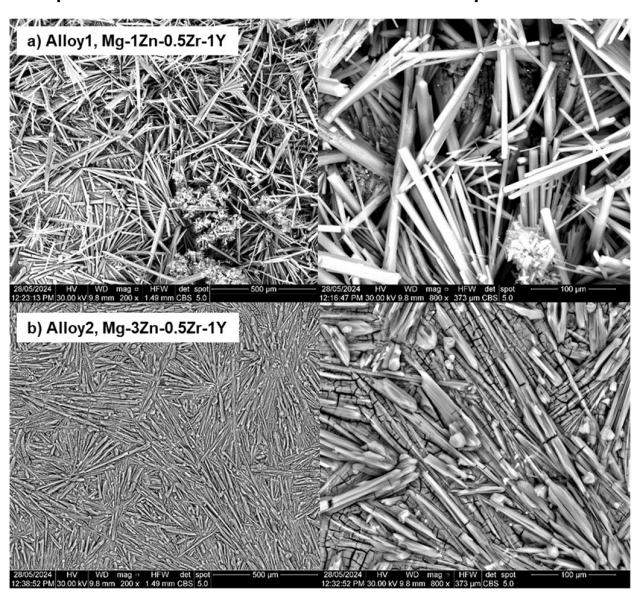


Figure 10: SEM images for a) Mg-1Zn-0.5Zr-1Y and b) Mg-3Zn-0.5Zr-1Y at 200x and 800x magnification after immersing in PBS solution for 7 days.

Table 4: Corrosion test results of six Mg-Zn-Zr-Y alloys.

Alloys	Corrosion Potential (V)	Corrosion Current Density (µA/cm²)	HER @10h (ml·cm²·hr ⁻¹)
1) Mg-1Zn-0.5Zr-1Y	-1.552	4.079	0.1164
2) Mg-3Zn-0.5Zr-1Y	-1.521	1.768	0.0167
3) Mg-5Zn-0.5Zr-1Y	-1.527	14.436	0.0336
4) Mg-3Zn-0.25Zr-1Y	-1.540	2.118	0.0423
5) Mg-3Zn-0.75Zr-1Y	-1.547	7.098	0.0199
6) Mg-3Zn-1Zr-1Y	-1.529	1.023	0.0179

5. DISCUSSION

5.1 Microstructure and Mechanical Characterisation

The microstructure of the Mg-Zn-Zr-Y alloys was analysed to understand the impact of alloying elements on grain refinement and phase formation. Alloy 2 (Mg-3Zn-0.5Zr-1Y) demonstrated a uniform grain structure with well-distributed intermetallic phases, contributing to its superior mechanical properties. The presence of zinc (Zn) and zirconium (Zr) played crucial roles in achieving this microstructural refinement [7][8][27]. Zinc, known for its ability to enhance grain refinement through the formation of Mg-Zn intermetallic compounds, contributed to the uniformity and stability of the microstructure [29]. This effect of zinc is well-documented, as studies have shown that Zn not only promotes grain refinement but also enhances the mechanical properties of magnesium alloys by improving their yield strength and ductility. However, excessive zinc can significantly reduce ductility. This is demonstrated in Alloy 3 (Mg-5Zn-0.5Zr-1Y), which has a yield strength of 88.56 MPa and an elongation of 4.17%, compared to Alloy 2, which has a yield strength of 80.72 MPa and an elongation of 11.78%. The higher zinc content in Alloy 3 leads to a heterogeneous distribution of phases and increased brittleness. Similar findings in the literature [30], indicate that high zinc levels can form coarse and continuous phases at grain boundaries, compromising ductility and overall mechanical performance.

Zirconium's influence in Alloy 2 was also significant. It acted as a potent grain refiner, preventing excessive grain growth during processing and contributing to the uniform grain structure observed in Alloy 2. Adding zirconium typically results in the formation of fine and uniformly distributed intermetallic phases, which are essential for enhancing the mechanical integrity and corrosion resistance of magnesium alloys [31]. This is supported by research indicating that Zr additions lead to improved mechanical properties due to their impact on grain boundary strengthening [7].

Furthermore, yttrium (Y) played a pivotal role in enhancing the age-hardening response and overall strength of Alloy 2. The synergistic effects of Zn, Zr, and Y not only improved the mechanical properties but also contributed to the alloy's enhanced corrosion resistance, making it an ideal candidate for biomedical applications where both high strength and superior corrosion resistance are required. This is in line with findings from other studies that have highlighted the beneficial impact of yttrium on the mechanical and corrosion properties of magnesium alloys [6].

The hardness values for the six Mg-Zn-Zr-Y alloys as depicted in Figure 7 generally fall within a narrow range of approximately 48.6 HV to 51.5 HV. This indicates that despite the variations in composition, the alloys exhibit similar hardness levels. Overall, the hardness values suggest that all alloys have been optimised to achieve a balance between hardness and other mechanical properties. The small variations in hardness indicate that the primary differences among the alloys lie in other mechanical properties such as tensile strength and ductility rather than in hardness alone. Previous studies have also observed that slight variations in alloy composition do not significantly affect hardness, further supporting this finding [32].

Overall, the yield strength of Alloy 2 (80.72 MPa) surpasses that of natural bone (51-66 MPa) [24], providing the necessary mechanical strength required for load-bearing biomedical applications. Additionally, the Young's modulus of Alloy 2 (39.41 GPa) is similar to bone (17-20 GPa) [24], which helps minimize the risk of stress shielding. Stress shielding occurs when an implant is much stiffer than the bone, leading to bone resorption and weakening over time [33]. By matching the Young's modulus of the implant material to that of natural bone, Alloy 2 can better integrate with the surrounding tissue and maintain bone health.

5.2 Corrosion Behaviour Evaluation

The corrosion behaviours of the six Mg-Zn-Zr-Y alloys were evaluated through open circuit potential (OCP) measurements, polarisation tests, and hydrogen evolution rate testing. The results demonstrate varying degrees of corrosion resistance among the alloys.

The potentiodynamic polarisation curves for the six Mg-Zn-Zr-Y alloys, shown in Figure 8b, provide insights into their corrosion behaviours. Alloy 1 (Mg-1Zn-0.5Zr-1Y) has a corrosion current density of 4.079 μA/cm², indicating a higher corrosion rate. In contrast, Alloy 2 (Mg-3Zn-0.5Zr-1Y) exhibits a lower current density of 1.768 μA/cm², demonstrating superior corrosion resistance. However, Alloy 3 (Mg-5Zn-0.5Zr-1Y) has a much higher current density of 14.436 μA/cm², indicating that further increasing Zn content beyond 3 wt% further reduced corrosion resistance. This indicates that while the optimal zinc content in Alloy 2 promotes the formation of a stable and protective oxide layer, the excessive zinc in Alloy 3 has adverse effects. This is likely due to the formation of continuous and coarse intermetallic phases that weaken the protective layer. Literature supports this phenomenon, showing that high zinc content can negatively impact corrosion resistance by forming less protective and more reactive intermetallic phases. [3].

Corrosion potential (OCP) and corrosion current density (i_{corr}) are both crucial in understanding the corrosion behaviours of alloys, but they reflect different aspects of the corrosion process. The OCP measures the thermodynamic tendency of a material to corrode; more positive values generally indicate higher resistance to corrosion initiation[23][34]. Alloy 2, with its more positive OCP value of -1.521 V, indicates the highest resistance to corrosion initiation among the tested alloys. This is attributed to the optimal combination of Zn and Zr, enhancing the formation of a stable and protective oxide layer, thereby improving the alloy's passivation behaviour [6][10].

When comparing these results to those of other magnesium alloys commonly used in medical applications, Alloy 2 demonstrates a distinct advantage. In comparison, Alloy AZ91 has an OCP value of around -1.55 V and a higher current density than Alloy 2, indicating that Alloy 2 provides superior corrosion resistance [25].

The hydrogen evolution rate measurements provide further insight into the corrosion behaviours of the alloys. Alloy 1 exhibited the highest hydrogen evolution rate, reaching up to 0.237 ml·cm²·hr⁻¹, indicating the highest corrosion rate. In contrast, Alloy 2 showed the lowest hydrogen evolution rate, as low as 0.0167 ml·cm²·hr⁻¹ at the 10-hour immersion period. This result demonstrates Alloy 2's superior corrosion resistance and aligns with the OCP and polarisation data.

The SEM analysis of corroded Alloy 1 and Alloy 2 after immersion in PBS solutions for 7 days further supports these findings. Alloy 1 shows significant white corrosion products, indicating more severe corrosion, while Alloy 2 displays fewer corrosion products, suggesting better corrosion resistance. The SEM images of Alloy 1 reveal extensive needle-like corrosion products and a porous surface, indicative of severe chemical reactions and corrosion. In contrast, the SEM images of Alloy 2 show a more stable and uniform surface with fewer needle-like structures. The surface appears less porous and more intact, correlating with the lower corrosion rates indicated by the hydrogen evolution and electrochemical testing. This suggests that Alloy 2 has better corrosion resistance, forming more protective and stable corrosion products compared to Alloy 1.

In addition to mechanical and corrosion properties, the financial costs and fabrication processes for Mg-Zn-Zr-Y alloys are critical considerations for practical application. Magnesium's sensitivity and reactivity necessitate protective atmospheres and special handling during fabrication to prevent oxidation and maintain material integrity, thereby increasing manufacturing costs compared to conventional materials. Despite higher initial

costs, the long-term benefits of Mg-Zn-Zr-Y alloys in biomedical applications, particularly Alloy 2, justify the investment. These alloys offer superior biocompatibility, biodegradability, and mechanical properties, making them competitive with materials like titanium and stainless steel. Unlike non-degradable implants, magnesium alloys naturally degrade, eliminating the need for additional removal surgeries, potentially reducing healthcare costs and improving patient outcomes.

5.3 Limitations of this Study

This study has several limitations. Due to machining difficulties, mechanical tests were conducted on only one sample per alloy, restricting statistical analyses and potentially not capturing the full variability in mechanical properties. Future studies should investigate the reproducibility of mechanical properties such as yield strength and elongation across multiple samples and processing batches. Additionally, the corrosion tests were performed under controlled laboratory conditions, which may not accurately reflect the complex in vivo environment. Factors such as varying pH levels, body fluids, and mechanical stresses in the human body can significantly influence corrosion behaviour. Lastly, while this study focused on mechanical and corrosion properties, the biocompatibility and biological response of these alloys were not extensively investigated. Comprehensive biocompatibility studies, including cell viability assays, histological analysis, and in vivo implantation studies, are essential for ensuring the safe and effective use of these alloys in biomedical applications.

6. CONCLUSION & FUTURE WORK

6.1 Conclusion

The investigation into the six Mg-Zn-Zr-Y alloys has yielded significant insights into their microstructural, mechanical, and corrosion properties. This study has highlighted the crucial roles of zinc (Zn), zirconium (Zr), and yttrium (Y) in enhancing the performance characteristics of magnesium alloys. Among the developed alloys, Alloy 2 (Mg-3Zn-0.5Zr-1Y) has been identified as the most promising candidate. It exhibited a uniform fine grain structure, superior mechanical properties, and excellent corrosion resistance. The synergistic effects of Zn, Zr, and Y were instrumental in achieving a refined microstructure, increased yield strength, and improved ductility, making Alloy 2 well-suited for biomedical applications requiring both strength and durability.

Alloy 2 demonstrated the highest ultimate tensile strength (UTS) of 201.61 MPa, a yield strength of 80.72 MPa, and a Young's modulus of 39.41 GPa, along with good ductility with an elongation of 11.78, which is stronger than bone and having similar stiffness with it. The hardness values across the alloys were similar, with Alloy 2 having a slightly lower hardness of 49.2 HV compared to the others. Evaluations of corrosion resistance showed that Alloy 2 had a lower corrosion current density of 1.768 μA/cm² and a more positive open circuit potential (OCP) value of -1.521 V, indicating excellent resistance to corrosion initiation and propagation. Additionally, Alloy 2 showed the lowest hydrogen evolution rate, as low as 0.0167 ml·cm²·hr⁻¹ at the 10-hour period, further demonstrating its superior corrosion resistance.

These results highlight the potential of Alloy 2 as a viable material for biomedical applications, combining enhanced mechanical performance with excellent corrosion resistance.

6.2 Future Work

While the current study provides a comprehensive foundation, further research is necessary to optimise and extend the applicability of the Mg-Zn-Zr-Y alloys. Future work should focus on several key areas. Further research into additional alloying elements and heat treatment processes is advised to enhance the mechanical properties and customize the performance of the alloys for specific biomedical applications. Exploring surface treatments and coatings is crucial to boost the corrosion resistance and biocompatibility of the alloys, ensuring their safe and effective application in medical devices.

Additionally, studying the fatigue properties of the alloys under cyclic loading conditions is crucial to ensure their reliability and durability in load-bearing biomedical applications. Examining the biodegradation rates and the effects of degradation products on the human body is necessary to ensure the alloys' safety and efficacy as biodegradable implants.

Finally, advancing to clinical trials to assess the real-world performance of the most promising alloy compositions in medical implants is essential, focusing on patient outcomes and long-term safety. Addressing these areas will contribute to the development of Mg-Zn-Zr-Y alloys with optimised properties, paving the way for their broader adoption in the biomedical field. The insights gained from this study, along with subsequent research, will play a crucial role in advancing the application of magnesium alloys in medical devices, offering safer and more effective solutions for patients.

REFERENCES

- [1] J. Chen, L. Tan, X. Yu, I. P. Etim, M. Ibrahim, and K. Yang, "Mechanical properties of magnesium alloys for medical application: A review," Nov. 01, 2018, *Elsevier Ltd.* doi: 10.1016/j.jmbbm.2018.07.022.
- [2] R. K. Singh Raman, S. Jafari, and S. E. Harandi, "Corrosion fatigue fracture of magnesium alloys in bioimplant applications: A review," *Eng Fract Mech*, vol. 137, pp. 97–108, 2015, doi: 10.1016/j.engfracmech.2014.08.009.
- [3] A. Gungor and A. Incesu, "Effects of alloying elements and thermomechanical process on the mechanical and corrosion properties of biodegradable Mg alloys," *Journal of Magnesium and Alloys*, vol. 9, no. 1, pp. 241–253, 2021, doi: 10.1016/j.jma.2020.09.009.
- [4] Y. Shi, B. Yang, and P. K. Liaw, "Corrosion-resistant high-entropy alloys: A review," Feb. 01, 2017, MDPI AG. doi: 10.3390/met7020043.
- [5] X. Meng, Z. Jiang, S. Zhu, and S. Guan, "Effects of Sr addition on microstructure, mechanical and corrosion properties of biodegradable Mg–Zn–Ca alloy," *J Alloys Compd*, vol. 838, Oct. 2020, doi: 10.1016/j.jallcom.2020.155611.
- [6] D. K. Xu, W. N. Tang, L. Liu, Y. B. Xu, and E. H. Han, "Effect of Y concentration on the microstructure and mechanical properties of as-cast Mg-Zn-Y-Zr alloys," *J Alloys Compd*, vol. 432, no. 1–2, pp. 129–134, Apr. 2007, doi: 10.1016/j.jallcom.2006.05.123.
- [7] M. Sun, G. Wu, W. Wang, and W. Ding, "Effect of Zr on the microstructure, mechanical properties and corrosion resistance of Mg-10Gd-3Y magnesium alloy," *Materials Science and Engineering: A*, vol. 523, no. 1–2, pp. 145–151, Oct. 2009, doi: 10.1016/j.msea.2009.06.002.
- [8] Y. Ding, C. Wen, P. Hodgson, and Y. Li, "Effects of alloying elements on the corrosion behavior and biocompatibility of biodegradable magnesium alloys: a review," *J. Mater. Chem. B*, vol. 2, no. 14, pp. 1912–1933, 2014, doi: 10.1039/c3tb21746a.
- [9] M. V Kiselevsky *et al.*, "Biodegradable Magnesium Alloys as Promising Materials for Medical Applications (Review)," *Sovremennye tehnologii v medicine*, vol. 11, no. 3, p. 146, 2019, doi: 10.17691/stm2019.11.3.18.
- [10] E. Zhang, D. Yin, L. Xu, L. Yang, and K. Yang, "Microstructure, mechanical and corrosion properties and biocompatibility of Mg–Zn–Mn alloys for biomedical application," *Materials Science and Engineering: C*, vol. 29, no. 3, pp. 987–993, 2009, doi: 10.1016/j.msec.2008.08.024.
- [11] M. Pogorielov, E. Husak, A. Solodivnik, and S. Zhdanov, "Magnesium-based biodegradable alloys: Degradation, application, and alloying elements," *Interv Med Appl Sci*, vol. 9, no. 1, pp. 27–38, 2017, doi: 10.1556/1646.9.2017.1.04.

- [12] F. Witte, "The history of biodegradable magnesium implants: A review☆," *Acta Biomater*, vol. 6, no. 5, pp. 1680–1692, 2010, doi: 10.1016/j.actbio.2010.02.028.
- [13] D. Noviana, D. Paramitha, M. F. Ulum, and H. Hermawan, "The effect of hydrogen gas evolution of magnesium implant on the postimplantation mortality of rats," *J Orthop Translat*, vol. 5, pp. 9–15, 2016, doi: 10.1016/j.jot.2015.08.003.
- [14] H. Ben Amara *et al.*, "Magnesium implant degradation provides immunomodulatory and proangiogenic effects and attenuates peri-implant fibrosis in soft tissues," *Bioact Mater*, vol. 26, pp. 353–369, 2023, doi: 10.1016/j.bioactmat.2023.02.014.
- [15] L. J. Liu and M. Schlesinger, "Corrosion of magnesium and its alloys," *Corros Sci*, vol. 51, no. 8, pp. 1733–1737, 2009, doi: https://doi.org/10.1016/j.corsci.2009.04.025.
- [16] R. Zeng et al., "Review of studies on corrosion of magnesium alloys," Transactions of Nonferrous Metals Society of China, vol. 16, pp. s763–s771, 2006, doi: 10.1016/s1003-6326(06)60297-5.
- [17] A. Atrens, N. Winzer, and W. Dietzel, "Stress Corrosion Cracking of Magnesium Alloys," *Adv Eng Mater*, vol. 13, no. 1–2, pp. 11–18, 2011, doi: 10.1002/adem.200900287.
- [18] S. Jafari, S. E. Harandi, and Singh, "A Review of StressCorrosion Cracking and Corrosion Fatigue of Magnesium Alloys for Biodegradable Implant Applications," *JOM*, vol. 67, no. 5, pp. 1143–1153, 2015, doi: 10.1007/s118370151366z.
- [19] X. Chen, J. Zhou, Y. Qian, and L. Zhao, "Antibacterial coatings on orthopedic implants," *Mater Today Bio*, vol. 19, p. 100586, 2023, doi: 10.1016/j.mtbio.2023.100586.
- [20] M. S. Dargusch et al., "Improved biodegradable magnesium alloys through advanced solidification processing," Scr Mater, vol. 177, pp. 234–240, 2020, doi: 10.1016/j.scriptamat.2019.10.028.
- [21] G. L. Song and A. Atrens, "Corrosion Mechanisms of Magnesium Alloys," *Adv Eng Mater*, vol. 1, no. 1, pp. 11–33, 1999, doi: 10.1002/(sici)1527-2648(199909)1:1<11::aid-adem11>3.0.co;2-n.
- [22] E. Zhang and L. Yang, "Microstructure, mechanical properties and bio-corrosion properties of Mg–Zn–Mn–Ca alloy for biomedical application," *Materials Science and Engineering: A*, vol. 497, no. 1–2, pp. 111–118, 2008, doi: 10.1016/j.msea.2008.06.019.
- [23] J. Li, Z. Chen, J. Jing, and J. Hou, "Effect of yttrium modification on the corrosion behavior of AZ63 magnesium alloy in sodium chloride solution," *Journal of Magnesium and Alloys*, vol. 9, no. 2, pp. 613–626, 2021, doi: 10.1016/j.jma.2020.02.027.
- [24] J. Kundu, F. Pati, J. H. Shim, and D. W. Cho, "Rapid prototyping technology for bone regeneration," *Rapid Prototyping of Biomaterials: Techniques in Additive Manufacturing*, pp. 289–314, Jan. 2014, doi: 10.1016/B978-0-08-102663-2.00012-5.

- [25] F. Iranshahi, M. B. Nasiri, F. G. Warchomicka, and C. Sommitsch, "Corrosion behavior of electron beam processed AZ91 magnesium alloy," *Journal of Magnesium and Alloys*, vol. 8, no. 4, pp. 1314–1327, Dec. 2020, doi: 10.1016/j.jma.2020.08.012.
- [26] X. Liu, D. Shan, Y. Song, and E. hou Han, "Influence of yttrium element on the corrosion behaviors of Mg–Y binary magnesium alloy," *Journal of Magnesium and Alloys*, vol. 5, no. 1, pp. 26–34, Mar. 2017, doi: 10.1016/j.jma.2016.12.002.
- [27] D. Zander and N. A. Zumdick, "Influence of Ca and Zn on the microstructure and corrosion of biodegradable Mg–Ca–Zn alloys," *Corros Sci*, vol. 93, pp. 222–233, 2015, doi: 10.1016/j.corsci.2015.01.027.
- [28] R. Zeng, Y. Hu, S. Guan, H. Cui, and E. Han, "Corrosion of magnesium alloy AZ31: The influence of bicarbonate, sulphate, hydrogen phosphate and dihydrogen phosphate ions in saline solution," *Corros Sci*, vol. 86, pp. 171–182, 2014, doi: 10.1016/j.corsci.2014.05.006.
- [29] A. Bahmani, S. Arthanari, and K. S. Shin, "Corrosion behavior of Mg–Mn–Ca alloy: Influences of Al, Sn and Zn," *Journal of Magnesium and Alloys*, vol. 7, no. 1, pp. 38–46, Mar. 2019, doi: 10.1016/j.jma.2018.11.004.
- [30] H. R. Bakhsheshi-Rad et al., "Mechanical and bio-corrosion properties of quaternary Mg-Ca-Mn-Zn alloys compared with binary Mg-Ca alloys," *Mater Des*, vol. 53, pp. 283–292, 2014, doi: 10.1016/j.matdes.2013.06.055.
- [31] K. Gusieva, C. H. J. Davies, J. R. Scully, and N. Birbilis, "Corrosion of magnesium alloys: The role of alloying," Apr. 01, 2015, *Maney Publishing*. doi: 10.1179/1743280414Y.0000000046.
- [32] M. Mohedano *et al.*, "Characterization and corrosion behavior of binary Mg-Ga alloys," *Mater Charact*, vol. 128, pp. 85–99, Jun. 2017, doi: 10.1016/j.matchar.2017.03.040.
- [33] M. Niinomi and M. Nakai, "Titanium-based biomaterials for preventing stress shielding between implant devices and bone," 2011. doi: 10.1155/2011/836587.
- [34] S. E. Harandi, M. Mirshahi, S. Koleini, M. H. Idris, H. Jafari, and M. R. A. Kadir, "Effect of calcium content on the microstructure, hardness and in-vitro corrosion behavior of biodegradable mg-ca binary alloy," *Materials Research*, vol. 16, no. 1, pp. 11–18, Jan. 2013, doi: 10.1590/S1516-14392012005000151.
- [35] C. Gao *et al.*, "Dual alloying improves the corrosion resistance of biodegradable Mg alloys prepared by selective laser melting," *Journal of Magnesium and Alloys*, vol. 9, no. 1, pp. 305–316, Jan. 2021, doi: 10.1016/j.jma.2020.03.016.
- [36] B. Mingo *et al.*, "Corrosion of Mg-9Al alloy with minor alloying elements (Mn, Nd, Ca, Y and Sn)," *Mater Des*, vol. 130, pp. 48–58, Sep. 2017, doi: 10.1016/j.matdes.2017.05.048.
- [37] W. Zhang, M. Li, Q. Chen, W. Hu, W. Zhang, and W. Xin, "Effects of Sr and Sn on microstructure and corrosion resistance of Mg-Zr-Ca magnesium alloy for biomedical applications," *Mater Des*, vol. 39, pp. 379–383, 2012, doi: 10.1016/j.matdes.2012.03.006.

- [38] J. Kubásek, D. Vojtěch, J. Lipov, and T. Ruml, "Structure, mechanical properties, corrosion behavior and cytotoxicity of biodegradable Mg-X (X = Sn, Ga, In) alloys," *Materials Science and Engineering C*, vol. 33, no. 4, pp. 2421–2432, May 2013, doi: 10.1016/j.msec.2013.02.005.
- [39] R. C. Zeng, W. C. Qi, H. Z. Cui, F. Zhang, S. Q. Li, and E. H. Han, "In vitro corrosion of asextruded Mg-Ca alloys-The influence of Ca concentration," *Corros Sci*, vol. 96, pp. 23–31, Jul. 2015, doi: 10.1016/j.corsci.2015.03.018.
- [40] Y. liang CHENG, T. wei QIN, H. min WANG, and Z. ZHANG, "Comparison of corrosion behaviors of AZ31, AZ91, AM60 and ZK60 magnesium alloys," *Transactions of Nonferrous Metals Society of China (English Edition)*, vol. 19, no. 3, pp. 517–524, Jun. 2009, doi: 10.1016/S1003-6326(08)60305-2.
- [41] V. Bazhenov *et al.*, "Gallium-containing magnesium alloy for potential use as temporary implants in osteosynthesis," *Journal of Magnesium and Alloys*, vol. 8, no. 2, pp. 352–363, Jun. 2020, doi: 10.1016/j.jma.2020.02.009.
- [42] J. Yang, J. Peng, E. A. Nyberg, and F. S. Pan, "Effect of Ca addition on the corrosion behavior of Mg-Al-Mn alloy," *Appl Surf Sci*, vol. 369, pp. 92–100, Apr. 2016, doi: 10.1016/i.apsusc.2016.01.283.
- [43] W. Liu, F. Cao, L. Chang, Z. Zhang, and J. Zhang, "Effect of rare earth element Ce and La on corrosion behavior of AM60 magnesium alloy," *Corros Sci*, vol. 51, no. 6, pp. 1334–1343, Jun. 2009, doi: 10.1016/j.corsci.2009.03.018.
- [44] D. H. Cho, B. W. Lee, J. Y. Park, K. M. Cho, and I. M. Park, "Effect of Mn addition on corrosion properties of biodegradable Mg-4Zn-0.5Ca-xMn alloys," *J Alloys Compd*, vol. 695, pp. 1166–1174, 2017, doi: 10.1016/j.jallcom.2016.10.244.

APPENDICES

Appendix i: Characterised results of Magnesium alloys from literatures.

Reference	Chemical Composition	Young's Modulus (GPa)	Yield Strength (MPa)	Corrosion Rate (mm/yr)	Corrosion Potential (V)	Corrosion Current (μΑ/cm2)	Corrosion Resistance (Ω/cm2)	Hardness (HV)
[25]	Mg-9Al-1Zn	45	160	2.59	-1.55	39.03	280-585	
	Mg-1Zn-0.3Ca-1.1Mn				-1.49	75.5	192	
[22]	Mg-2Zn-0.5Ca-1.2Mn				-1.496	57.2	266	
	Mg-1.5Zn-1Ca-1.1Mn				-1.507	2.95	3621	
	Pure Mg			2.17	-2.03	30.9		27
	Mg-0.7Ca			1.479	-1.9	19.7		35
[2.4]	Mg-1Ca			1.876	-1.96	22.4		39
[34]	Mg-2Ca			2.017	-1.99	31.2		41
	Mg-3Ca			2.881	-2.05	39.5		46
	Mg-4Ca			3.604	-2.06	47		48
	Pure Mg		27.5		-2.027	370.7	820	28.9
	Mg-2Ca		47.3		-1.997	301.9	950	43.2
(0.0)	Mg-4Ca		34.5		-2.055	395.7	780	53.3
[30]	Mg-2Zn-2Ca-0.5Mn		78.3		-1.617	78.3	3260	64.5
	Mg-4Zn-2Ca-0.5Mn		83.1		-1.652	99.6	2380	69.1
	Mg-7Zn-2Ca-0.5Mn		45.4		-1.728	174.1	1440	82.2
	Mg-5.68Zn-0.78Zr		124					
[6]	Mg-5.53Zn-0.83Zr-1.08Y		163					
[6]	Mg-5.64Zn-0.73Zr-1.97Y		144					
	Mg-5.49Zn-0.82Zr-3.08Y		85					
	Pure Mg			2.874	-1.51	27.13		
	Mg-3Zn-0.2Ca-0.3Mn	34	57	0.078	-1.52	25.08		52.1
[3]	Mg-3Zn-1.8Ca-0.3Mn	48	58	0.126	-1.48	7.19		55
	Mg-5Zn-0.2Ca-0.3Mn	52	83	0.107	-1.43	70.3		54.9
	Mg-5Zn-1.8Ca-0.3Mn	50	67	0.068	-1.49	15.79		65.7
	Mg-6Al-1Zn			3.5	-1.5			
	Mg-6Al-1Zn-0.4Mn			1.4	-1.45			
[35]	Mg-6Al-1Zn-0.8Sn			1.2	-1.43			
	Mg-6Al-1Zn0.4Mn- 0.8Sn			0.9	-1.4			
	Mg-2Zn-0.3Ca			10	-1.79	192		45
	Mg-2Zn-0.3Ca-0.1Sr			10	-1.79	205		47
[5]	Mg-2Zn-0.3Ca-0.3Sr			20	-1.8	244		49
	Mg-2Zn-0.3Ca-0.5Sr			25	-1.82	327		51
	Mg-2Zn-0.3Ca-1Sr			15	-1.85	413		54
	Mg-9Al				-1.472	86		108
[36]	Mg-9Al-0.5Zr				-1.535	5.2		87
	Mg-9Al-0.25Nd				-1.485	43.4		87

	Mg-9Al-0.5Ca			-1.535	5.5		80
	Mg-9Al-0.5Y			-1.525	24		74
	Mg-9Al-1Sn			-1.525	45		79
	Mg-5Zn-1Ca			-1.89	508		79
[37]	Mg-5Zn-1Ca-4Sr-4Sn						
	Mg-0.6Ca		4 225	-1.78	42.6		
	Mg-0.8Zn-0.6Ca		1.335	-1.604	35		
[27]	Mg-1.8Zn-0.6Ca		0.124	-1.616	0.75		
[27]	Mg-0.8Zn-1.6Ca		0.196	-1.594	0.9		
	Mg-1.8Zn-1.6Ca		0.224	-1.628	1.5		
	Pure Mg		0.28	-1.584	2.5		
	Mg-1Sn		2.5				
	Mg-5Sn		0.5				
	Mg-7Sn		1.35				
	Mg-1Ga		1.5				
[38]	Mg-5Ga		0.2				
	Mg-7Ga		0.45				
	Mg-1In		0.9				
	Mg-5In		0.45				
	Mg-7In		0.6				
			0.65				
[20]	Mg-0.5Ca	160	0.80%				52
[39]	Mg-0.8Ca Mg-1.4Ca	190	0.70%				57
	Mg-3Y-10Gd	170	1%				53
	Mg-0.1Zr-3Y-10Gd			-1.61	1576		
	Mg-0.2Zr-3Y-10Gd			-1.56	1230		
	Mg-0.3Zr-3Y-10Gd			-1.55	191.4		
[7]	Mg-0.4Zr-3Y-10Gd			-1.53	18.6		
	Mg-0.5Zr-3Y-10Gd			-1.49	17.5		
	Mg-0.6Zr-3Y-10Gd			-1.47	14.7		
	Mg-1Zr-3Y-10Gd			-1.49	18.2		
	Mg-3Al-1Zn-0.2Mn			-1.54	22.1		
	Mg-9Al-0.7Zn-0.13Mn				488.6		
[40]					234.9		
	Mg-6Al-0.13Mn				156.7		
	Mg-5.5Zn-0.45Mn				10.03		
	Mg-4Zn-4Ga	160	0.2				
[41]	Mg-4Zn-0.2Ca-4Ga	158	0.35	-			
	Mg-4Zn-0.3Y-4Ga	140	0.25				
	Mg-4Zn-0.3Nd-4Ga	145	0.3	-			
	Mg-1Ga		1.47	-1.723			49
[32]	Mg-2Ga		1.45	-1.754			52
	Mg-3Ga		1.35	-1.764			51
	Mg-4Ga		1.26	-1.753			53
[26]	Mg-1Y			-1793	12.2	2128	
	Mg-2Y			-1.789	18	1440	

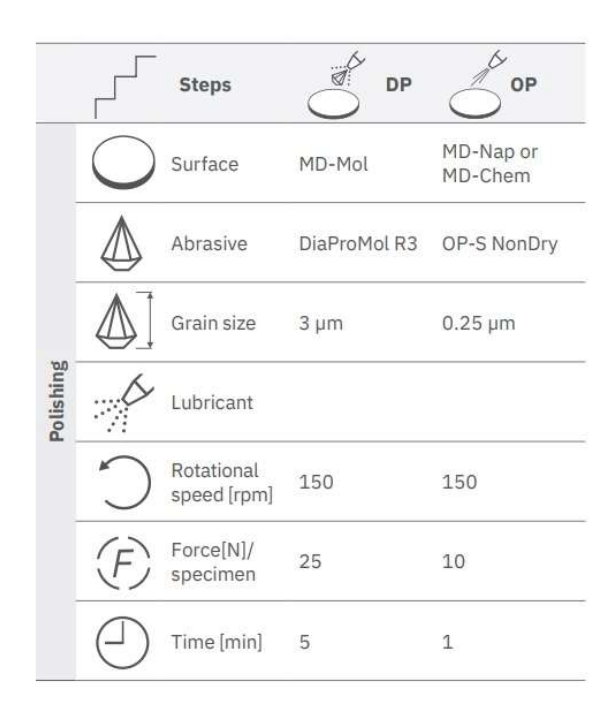
	Mg-3Y			-1.758	18.3	1419	
	Mg-4Y			-1.751	20	1303	
	Mg-6Al-3Zn			-1.635	119		
	Mg-6Al-3Zn-0.25Y			-1.648	74.5		
[23]	Mg-6Al-3Zn-0.5Y			-1.685	72.9		
	Mg-6Al-3Zn-0.75Y			-1.685	61.2		
	Mg-6Al-3Zn-1Y			-1.691	32.1		
	Mg-5Al-0.4Mn			-1.46	224.16		
	Mg-5Al-0.2Ca-0.4Mn			-1.59	38.6		
[42]	Mg-5Al-1Ca-0.4Mn			-1.58	46.5		
	Mg-5Al-2Ca-0.4Mn			-1.62	37.82		
	Mg-5Al-4Ca-0.4Mn			-1.48	258.35		
	Mg-6Al-0.2Mn			-1.508	26.47		
	Mg-6Al-0.2Mn-0.5Ce			-1.54	18.43		
	Mg-6Al-0.2Mn-1Ce			-1.574	11.35		
[43]	Mg-6Al-0.2Mn-2Ce			-1.562	15.2		
	Mg-6Al-0.2Mn-0.5La			-1.55	24.82		
	Mg-6Al-0.2Mn-1La			-1.565	23.02		
	Mg-6Al-0.2Mn-2La			-1.51	27.51		
	Mg-4Zn-0.5Ca			-1.527	8.849	4646	
[44]	Mg-4Zn-0.5Ca-0.4Mn			-1.473	4.148	5300	
	Mg-4Zn-0.5Ca-0.8Mn			-1.414	2.857	7010	
	Mg-0.7Ca-0.5Mn		1.69	-1.552	28.1		79
[20]	Mg-2Al-0.7Ca-0.5Mn		8.66	-1.452	67.3		90
[29]	Mg-9Sn-0.7Ca-0.5Mn		8.77	-1.522	88.5		70
	Mg-4Zn-0.7Ca-0.5Mn		3.63	-1.518	20.1		88
_	Mg-1Zn-1Mn	250		-1.47			
[10]	Mg-2Zn-1Mn	251		-1.46			
	Mg-3Zn-1Mn	270		-1.54	·		

Appendix ii: Polishing method for magnesium alloys.

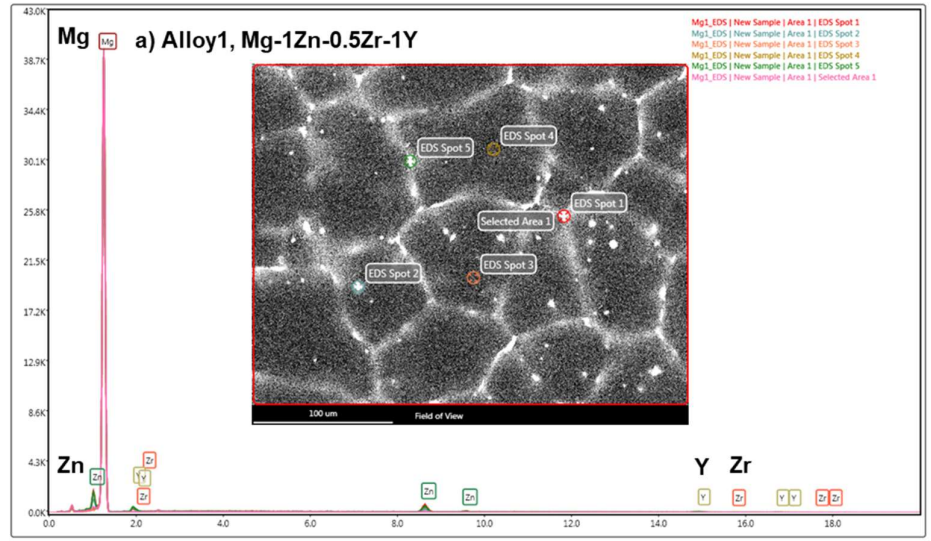
Metalog Method – example MgAl alloy, cast

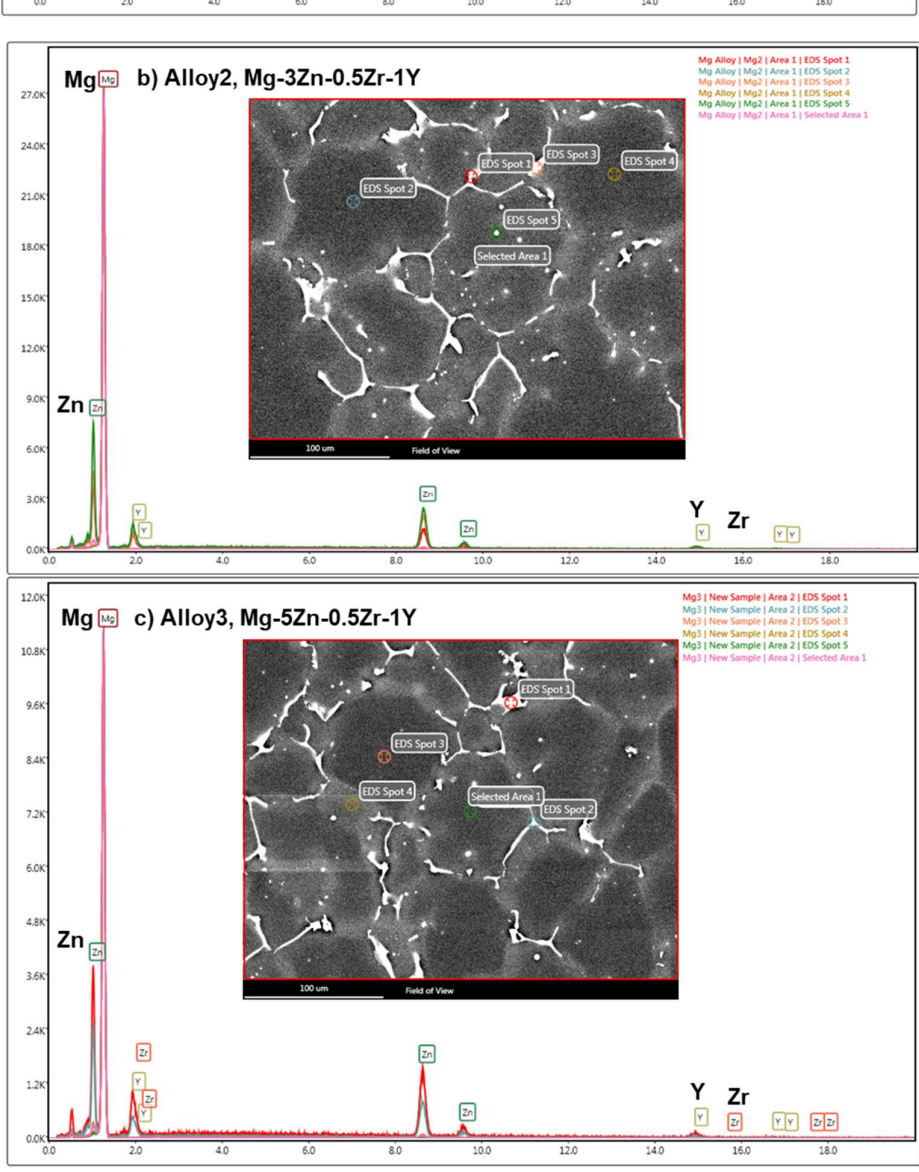
A

	7	Steps	PG	FG	
Grinding	\bigcirc	Surface	SiC-Foil	MD-Largo	
	\triangle	Abrasive	SiC	DiaPro AllegroLargo 9	
		Grain size	#320	9 μm	
		Lubricant	Water		
	\mathbb{C}	Rotational speed [rpm]	300	150	
	(F)	Force[N]/ specimen	25	40	
		Time [min]	Until plane	3	

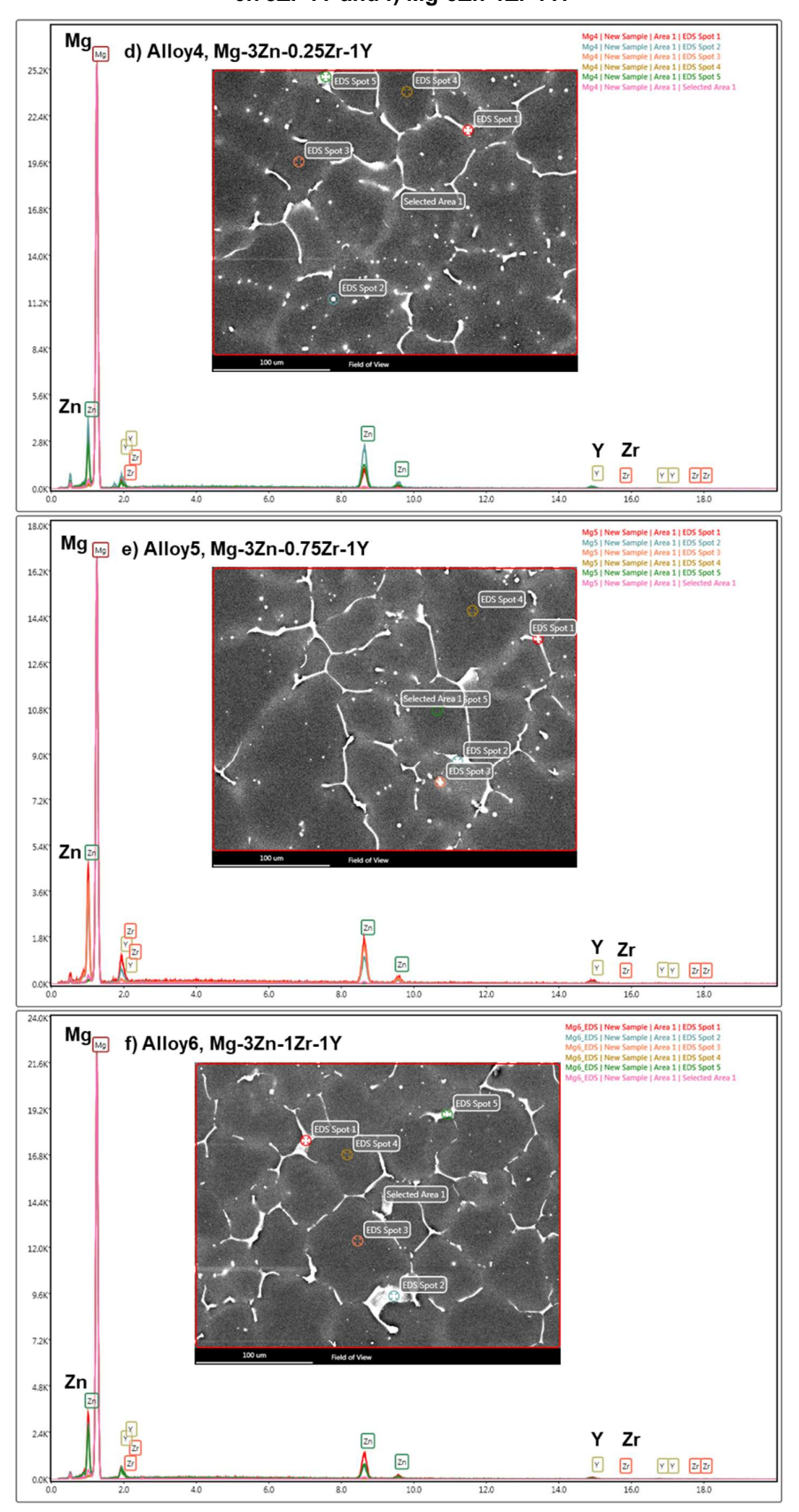


Appendix iii: EDS spectrum analysis EDS spectrum analysis of a) Mg-1Zn-0.5Zr-1Y, b) Mg-3Zn-0.5Zr-1Y and c) Mg-5Zn-0.5Zr-1Y.





Appendix iv: EDS spectrum analysis EDS spectrum analysis of d) Mg-3Zn-0.25Zr-1Y, e) Mg-3Zn-0.75Zr-1Y and f) Mg-3Zn-1Zr-1Y.



Appendix v: Vickers hardness test results.

	Vickers Hardness (HV)							
Indent No.	Mg-1Zn-0.5Zr-1Y	Mg-3Zn-0.5Zr-1Y	Mg-5Zn-0.5Zr-1Y	Mg-3Zn-0.25Zr-1Y	Mg-3Zn-0.75Zr-1Y	Mg-3Zn-1Zr-1Y		
1	52	47.8	55	54.6	51.2	48		
2	51.4	45.8	51.2	57.1	49.5	45.6		
3	55.7	47.8	50.8	52.9	52.9	44.3		
4	48.6	46.8	53.5	45.6	49.3	52.7		
5	49.9	54.8	48.9	54.6	45.1	49.1		
6	48	47.5	47.3	51	52.9	50.3		
7	49.7	50.1	53.9	49.1	50.1	47.8		
8	52.5	52.9	49.3	47	55.5	50.8		
Mean	51.0	49.2	51.2	51.5	50.8	48.6		
Std Dev	2.483	3.162	2.707	4.029	3.117	2.759		

Appendix vi: a) Mg-1Zn-0.5Zr-1Y and b) Mg-3Zn-0.5Zr-1Y after immersed in PBS for 7 days.

